



Observation of J/ψ -pair production in pp collisions at $\sqrt{s} = 7 \text{ TeV}$ [☆]

LHCb Collaboration

ARTICLE INFO

Article history:

Received 6 September 2011

Received in revised form 6 December 2011

Accepted 6 December 2011

Available online 9 December 2011

Editor: M. Doser

ABSTRACT

The production of J/ψ pairs in proton–proton collisions at a centre-of-mass energy of 7 TeV has been observed using an integrated luminosity of 37.5 pb^{-1} collected with the LHCb detector. The production cross-section for pairs with both J/ψ in the rapidity range $2 < y^{J/\psi} < 4.5$ and transverse momentum $p_T^{J/\psi} < 10 \text{ GeV}/c$ is

$$\sigma^{J/\psi J/\psi} = 5.1 \pm 1.0 \pm 1.1 \text{ nb},$$

where the first uncertainty is statistical and the second systematic.

© 2011 CERN. Published by Elsevier B.V. Open access under [CC BY-NC-ND license](http://creativecommons.org/licenses/by-nc-nd/3.0/).

1. Introduction

The mechanism of heavy quarkonium production is a long-standing problem in QCD. An effective field theory, non-relativistic QCD (NRQCD), provides the foundation for much of the current theoretical work. According to NRQCD, the production of heavy quarkonium factorises into two steps: a heavy quark–antiquark pair is first created perturbatively at short distances and subsequently evolves non-perturbatively into quarkonium at long distances. The NRQCD calculations depend on the colour-singlet (CS) and colour-octet (CO) matrix elements, which account for the probability of a heavy quark–antiquark pair in a particular colour state to evolve into heavy quarkonium.

Leading order (LO) calculations in the CS model [1–3] were first used to describe experimental data. However, they underestimate the observed cross-section for single J/ψ production at high p_T at the Tevatron [4]. To resolve this discrepancy the CO mechanism was introduced [5]. The corresponding matrix elements were determined from the large- p_T data as the CO cross-section falls more slowly than the CS one. However, recent calculations [6–9] close the gap between the CS predictions and the experimental data [10] reducing the need for large CO contributions. Thus, further experimental tests are needed. Pair production of quarkonium can cast light on this problem as this process depends heavily on the production mechanism. For both the CS and CO models, contributions from double parton scattering [11–13] could potentially be significant.

The only observation of charmonia pair production in hadronic collisions to date was by the NA3 Collaboration, who found evidence for J/ψ pair production in multi-muon events in pion–platinum interactions at pion momenta of 150 and 280 GeV/c [14]

and in proton–platinum interactions at a proton momentum of 400 GeV/c [15]. The cross-section ratio $\sigma^{J/\psi J/\psi}/\sigma^{J/\psi}$ was measured to be $(3 \pm 1) \times 10^{-4}$ for pion-induced production, where $\sigma^{J/\psi}$ is the inclusive J/ψ production cross-section. At NA3 energies the main contribution to the J/ψ pair cross-section arises from the quark–antiquark annihilation channel [16]. This is not the case for proton–proton collisions at the LHC, where the gluon–gluon fusion process dominates [17,18].

Theoretical calculations based on the LO production of CS-states predict that the total cross-section for J/ψ -pair production in proton–proton interactions at $\sqrt{s} = 7 \text{ TeV}$ is equal to 24 nb [19,20]. These calculations take into account $J/\psi J/\psi$, $J/\psi \psi(2S)$ and $\psi(2S) \psi(2S)$ production but do not include the possible contribution from double parton scattering. In the rapidity interval $2.0 < y^{J/\psi} < 4.5$, relevant to the LHCb experiment, the expected value is 4 nb with an uncertainty of around 30%. At small invariant masses of the J/ψ pair a tetraquark state, built from four c -quarks, may exist [20] and would be visible as a narrow resonance in the mass spectrum.

2. The LHCb detector and dataset

The LHCb detector is a forward spectrometer [21] providing charged particle reconstruction in the pseudorapidity range $1.9 < \eta < 4.9$. The detector elements are placed along the beam line of the LHC starting with the Vertex Locator, a silicon strip device that surrounds the proton–proton interaction region. This reconstructs precisely the locations of interaction vertices, the locations of decays of long-lived hadrons and contributes to the measurement of track momenta. Other detectors used to measure track momenta comprise a large area silicon strip detector located upstream of a dipole magnet with bending power around 4 Tm and a combination of silicon strip detectors and straw drift-tubes placed downstream. Two ring imaging Cherenkov detectors are used to

[☆] © CERN for the benefit of the LHCb Collaboration.

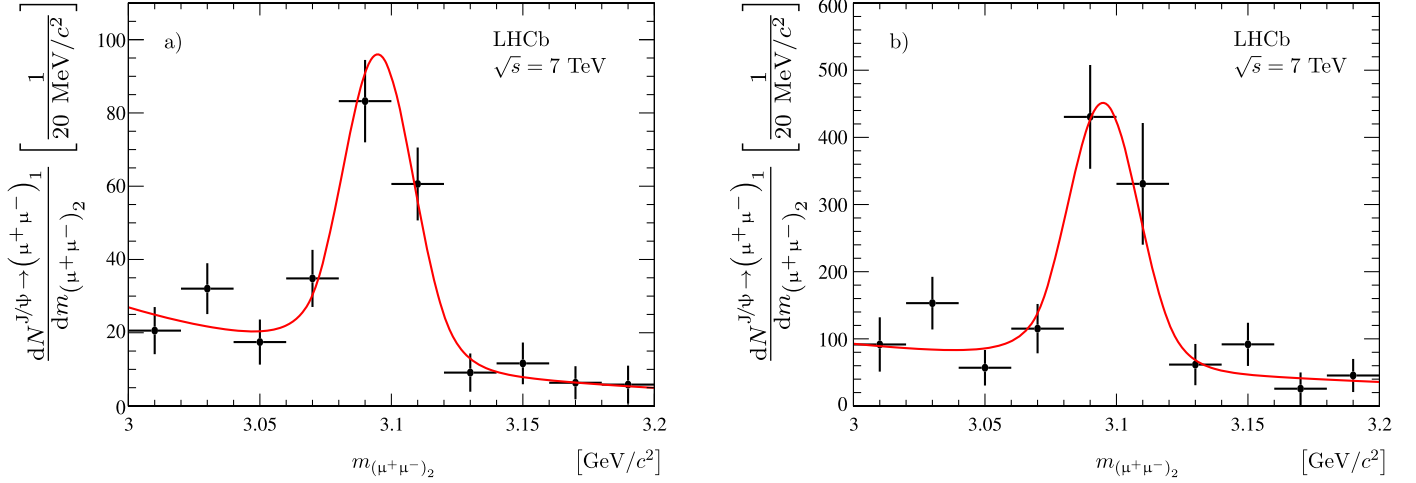


Fig. 1. The fitted yields of $J/\psi \rightarrow (\mu^+\mu^-)_1$ in bins of $(\mu^+\mu^-)_2$ invariant mass: (a) the raw signal yield observed in the data; (b) the efficiency-corrected yield (Section 6). The result of a fit with a double-sided Crystal Ball function for the signal and an exponential background is superimposed.

identify charged hadrons. Further downstream, an electromagnetic calorimeter is used for photon and electron identification, followed by a hadron calorimeter and a muon system consisting of alternating layers of iron and chambers (MWPC and triple-GEM) that distinguishes muons from hadrons. The calorimeters and muon system provide the capability of first-level hardware triggering.

The LHCb trigger system consists of three levels. The first level (L0) is designed to reduce the LHC bunch crossing rate of 40 MHz to a maximum of 1 MHz, at which the complete detector is read out. This is the input to the first stage of the software trigger, which performs a partial event reconstruction to confirm or discard the L0 trigger decision. The second stage of the software trigger performs a full event reconstruction to further discriminate signal events from other pp collisions. To avoid that a few events with high occupancy dominate the CPU time, a set of global event cuts is applied on the hit multiplicities of each sub-detector used by the pattern recognition algorithms. These cuts were chosen to reject high-multiplicity events with a large number of pp interactions with minimal loss of luminosity.

The data used for this analysis comprise an integrated luminosity of 37.5 pb^{-1} of pp collisions at a centre-of-mass energy of 7 TeV collected by the LHCb experiment between July and November 2010. This number includes the dead-time of trigger and data acquisition systems. During this period all detector components were fully operational and in a stable condition. The mean number of visible proton–proton collisions per bunch crossing was up to 2.5.

The simulation samples used are based on the PYTHIA 6.4 generator [22] configured with the parameters detailed in Ref. [23]. The EVTGEN [24] and GEANT4 [25] packages are used to generate hadron decays and simulate interactions in the detector, respectively. Prompt charmonium production is generated in PYTHIA according to the leading order CS and CO mechanisms.

3. Event selection and signal yield

In this analysis the J/ψ is reconstructed through its decay into a pair of muons. Events with at least four muons are selected. $J/\psi \rightarrow \mu^+\mu^-$ candidates are formed from pairs of oppositely-charged particles identified as muons that each have a transverse momentum greater than 650 MeV/c and that originate from a common vertex. Track quality is ensured by requiring that the $\chi^2_{\text{tr}}/\text{ndf}$ provided by the track fit is less than five. Well identified muons are selected by requiring that the difference in logarithms of the global likelihood

of the muon hypothesis, provided by the particle identification detectors [26], with respect to the hadron hypothesis, $\Delta \ln \mathcal{L}^{\mu-h}$, be greater than zero. To suppress the contribution from duplicate particles created by the reconstruction procedure, if two muon candidates have a symmetrised Kullback–Leibler divergence [27] less than 5000, only the particle with the best track fit is considered.

Selected $\mu^+\mu^-$ candidates with an invariant mass in the range $3.0 < m_{\mu^+\mu^-} < 3.2 \text{ GeV}/c^2$ are paired to form $(\mu^+\mu^-)_1(\mu^+\mu^-)_2$ combinations. A fit of the four-muon candidate is performed [28] that requires the four tracks to be consistent with originating from a common vertex and that this vertex is compatible with one of the reconstructed pp collision vertices. To reject background where two J/ψ candidates originate from different pp collisions, the reduced χ^2 of this fit, χ^2/ndf , is required to be less than five.

The number of events with two J/ψ mesons is extracted from the single J/ψ mass spectra. The invariant mass distributions of the first muon pair are obtained in bins of the invariant mass of the second pair.¹ The single J/ψ mass spectrum is modelled empirically using simulated events. This exhibits non-Gaussian tails on either side of the peak. The tail on the left-hand side is dominated by radiative effects in J/ψ decay, while the right-hand side tail is due to non-Gaussian effects in the reconstruction. The shape of the distribution is described by a function that is similar to a Crystal Ball function [29,30], but with the power-law tails on both sides of the core Gaussian component. The position of the J/ψ peak, the effective mass resolution and the tail parameters of this double-sided Crystal Ball function are fixed to the values determined from an analysis of the signal shape in the inclusive J/ψ sample. Combinatorial background is modelled using an exponential function. This model is used to extract the yield of $J/\psi \rightarrow (\mu^+\mu^-)_1$ in bins of the $(\mu^+\mu^-)_2$ invariant mass. The extracted yield is shown in Fig. 1(a) together with the result of a fit according to the model described above. The yield of events with double J/ψ production given by the fit is $N^{J/\psi} = 141 \pm 19$, where the statistical significance of this signal exceeds 6σ . A fit with position and resolution of the signal peak left free was also performed and gave consistent results.

Studies of single J/ψ production indicate that the detector acceptance and efficiency is high for the fiducial range $2 < y^{J/\psi} < 4.5$ and $p_{\text{T}}^{J/\psi} < 10 \text{ GeV}/c$. The raw yield of events with both J/ψ mesons within this range is 139 ± 18 . The yield of events with

¹ The $\mu^+\mu^-$ pair with lower transverse momentum is chosen to be the first pair.

both J/ψ mesons in the fiducial range and explicitly triggered by one of the J/ψ candidates through the single muon or dimuon trigger lines [31], is found to be 116 ± 16 . This sample is considered for the determination of the production cross-section.

The contribution to the yield from the pileup of two interactions each producing a single J/ψ meson is estimated using simulation together with the measured J/ψ production cross-section [32]. This study shows that for the 2010 data-taking conditions the background from this source is expected to be less than 1.5 events and hence can be neglected. In a similar way the contribution to the yield from events with J/ψ mesons originating from the decays of beauty hadrons is found to be negligible.

4. Efficiency evaluation

The per-event efficiency for a J/ψ -pair event, $\varepsilon_{J/\psi}^{\text{tot}}$, is decomposed into three factors,

$$\varepsilon_{J/\psi}^{\text{tot}} = \varepsilon_{J/\psi}^{\text{reco}} \times \varepsilon_{J/\psi}^{\mu\text{ID}} \times \varepsilon_{J/\psi}^{\text{trg}}, \quad (1)$$

where $\varepsilon_{J/\psi}^{\text{reco}}$ is the product of the (geometrical) acceptance with reconstruction and selection efficiency, $\varepsilon_{J/\psi}^{\mu\text{ID}}$ is the efficiency for muon identification and $\varepsilon_{J/\psi}^{\text{trg}}$ is the trigger efficiency for reconstructed and selected events.

The efficiency for the acceptance, reconstruction and selection for the two J/ψ mesons is factorised into the product of efficiencies for the first and second J/ψ ,

$$\varepsilon_{J/\psi}^{\text{reco}} = \varepsilon_{J/\psi}^{\text{reco}}(p_T^{J/\psi_1}, y^{J/\psi_1}, |\cos \vartheta_{J/\psi_1}^*|) \times \varepsilon_{J/\psi}^{\text{reco}}(p_T^{J/\psi_2}, y^{J/\psi_2}, |\cos \vartheta_{J/\psi_2}^*|). \quad (2)$$

The single J/ψ efficiency $\varepsilon_{J/\psi}^{\text{reco}}$ is a function of the transverse momentum p_T , rapidity y and $|\cos \vartheta^*|$, where ϑ^* is the angle between the μ^+ momentum in the J/ψ centre-of-mass frame and the J/ψ flight direction in the laboratory frame. It is evaluated using simulation. The validity of the factorisation hypothesis of Eq. (2) is checked with simulation and based on these studies a correction factor of 0.975 is applied to $\varepsilon_{J/\psi}^{\text{reco}}$. For the simulated data of single prompt J/ψ production the cut on the muon likelihood is not applied and that on $\chi^2(J/\psi)/\text{ndf}$ is replaced with a similar cut on the single J/ψ , $\chi^2(J/\psi)/\text{ndf} < 5$. The efficiency of the cut on χ^2/ndf is estimated from the data and compared to the simulation. Based on these studies a correction factor of 1.026 is applied to $\varepsilon_{J/\psi}^{\text{reco}}$, and a systematic uncertainty of 3% is assigned. The efficiency $\varepsilon_{J/\psi}^{\text{reco}}$ is also corrected by a factor 1.024 ± 0.011 [32], that accounts for the ratio of the reconstruction efficiency of the muon detector observed in the data compared to the simulation.

The muon identification efficiency is extracted from the analysis of the inclusive J/ψ sample. Two efficiencies are evaluated: the single muon identification efficiency $\varepsilon_{\mu}^{\mu\text{ID}}$ and the J/ψ efficiency $\varepsilon_{J/\psi}^{\mu\text{ID}}$. Both are measured as a function of the value of the cut made on $\Delta \ln \mathcal{L}^{\mu-h}$. The squared efficiency $(\varepsilon_{1\mu}^{\mu\text{ID}})^2$ and $\varepsilon_{J/\psi}^{\mu\text{ID}}$ are found to be equal to better than one per mille. The value of $\varepsilon_{J/\psi}^{\mu\text{ID}} = (\varepsilon_{1\mu}^{\mu\text{ID}})^2 = (91.0 \pm 0.1)\%$ has been used as a global factor for the evaluation of the total efficiency using Eq. (1). As a cross-check, the efficiency of the muon identification for J/ψ pairs has been estimated from the signal itself. Though statistically limited, the value is consistent with that given above.

The trigger efficiency is calculated to be

$$\varepsilon_{J/\psi}^{\text{trg}} = 1 - (1 - \varepsilon_{J/\psi}^{\text{trg}}(p_T^{J/\psi_1}, y^{J/\psi_1})) \times (1 - \varepsilon_{J/\psi}^{\text{trg}}(p_T^{J/\psi_2}, y^{J/\psi_2})).$$

The trigger efficiency for a single J/ψ , $\varepsilon_{J/\psi}^{\text{trg}}$, is determined directly on data from the inclusive prompt J/ψ sample as a function of p_T and rapidity y . The efficiency is determined by classifying an event which would also have been triggered without the J/ψ as TIS (Trigger Independent of Signal), and/or classifying the event where the J/ψ alone is sufficient to trigger the event as a TOS (Trigger On Signal) event [33,34]. The LHCb trigger system records all the information needed for such classification. Events can be classified as TIS and TOS simultaneously (TIS & TOS), which allows the extraction of the trigger efficiency relative to the off-line reconstructed and selected events from data alone

$$\varepsilon_{J/\psi}^{\text{trg}} = \frac{N^{\text{TIS \& TOS}}}{N^{\text{TIS}}},$$

where N^{TIS} is the number of TIS events, and $N^{\text{TIS \& TOS}}$ is the number of events that are simultaneously TIS and TOS. The method has been cross-checked using Monte Carlo simulation.

The effect of the global event cuts applied in the trigger has been studied in detail for inclusive J/ψ events in Ref. [32]. Since the sub-detector hit multiplicity observed in single and double J/ψ events is similar, the efficiency of the global event cuts, $(93 \pm 2)\%$, is taken from that study and applied to $\varepsilon_{J/\psi}^{\text{trg}}$.

For selected J/ψ -pair events the mean value of $\varepsilon_{J/\psi}^{\text{reco}}$ is 31% and it varies from 0.8% to 70%. The mean value for $\varepsilon_{J/\psi}^{\text{trg}}$ is 85% and it varies from 61% to 93%.

5. Systematic uncertainties

Systematic uncertainties affecting the cross-section measurement have been evaluated properly taking correlations into account where appropriate. The dominant source of systematic uncertainty is due to the knowledge of the track-finding efficiency. An uncertainty of 4% per track is assigned based on studies comparing the reconstruction efficiency in data and simulation using a tag and probe approach [34].

The second major source of uncertainty is due to the evaluation of the trigger efficiency. The method discussed in Section 4 has been cross-checked in several ways, in particular, by using events triggered by the first or second J/ψ only. The observed differences lead to the assignment of an 8% systematic uncertainty.

A further source of uncertainty is the determination of the per-event efficiency defined by Eq. (1). This is estimated to be 3% by varying the uncertainties of the various factors entering into Eq. (1).

The unknown polarisation of J/ψ mesons affects the acceptance, reconstruction and selection efficiency $\varepsilon_{J/\psi}^{\text{reco}}$ [32]. In this analysis the effect is reduced by explicitly taking into account the dependence of the acceptance on $|\cos \vartheta^*|$ in the efficiency determination (Eq. (2)). The remaining dependence results in a systematic uncertainty of 5% per J/ψ .

Additional systematic uncertainties arise due to the difference observed between the data and simulation for the behaviour of the cut on χ^2 (3%), the global event cuts (2%), and uncertainty of 1.1% per J/ψ associated with the efficiency for muon identification, as discussed in Section 4. The systematic uncertainties associated with the other selection criteria and the J/ψ lineshape parametrisation are negligible.

The luminosity was measured at specific periods during the data taking using both van der Meer scans [35] and a beam-gas imaging method [36]. The instantaneous luminosity determination is then based on a continuous recording of the multiplicity of tracks reconstructed in Vertex Locator, which has been normalised to the absolute luminosity scale. Consistent results are found for

Table 1

Relative systematic uncertainties on the cross-section measurement. The total uncertainty is calculated as the quadratic sum of the individual components.

Source	Systematic uncertainty [%]
Track-finding efficiency	4×4
Trigger efficiency	8
Per-event efficiency	3
J/ψ polarisation	2×5
Data/simulation difference for χ^2/ndf	3
Global event cuts	2
Muon identification	2×1.1
Luminosity	3.5
J/ψ → μ ⁺ μ ⁻ branching ratio	2×1
Total	21

the absolute luminosity scale with a precision of 3.5%, dominated by the beam current uncertainty [37,38].

The relative systematic uncertainties are summarised in Table 1, where the total uncertainty is defined as the quadratic sum of the individual components.

6. Cross-section determination

The efficiency-corrected yield for events with both J/ψ candidates in the fiducial region is extracted using the procedure discussed in Section 3. To account for the efficiency a weight ω , defined as

$$\omega^{-1} = \varepsilon_{J/\psi J/\psi}^{\text{tot}}$$

where $\varepsilon_{J/\psi J/\psi}^{\text{tot}}$ is the total efficiency defined in Eq. (1), is applied to each candidate in the sample.

The corrected yield of J/ψ → (μ⁺μ⁻)₁ in bins of (μ⁺μ⁻)₂ invariant mass is shown in Fig. 1(b). As previously described, to extract the yield a fit with a double-sided Crystal Ball function for the signal, together with an exponential function for the background component, is performed. Again, the position of the J/ψ peak and the effective mass resolution are fixed to the values found in the inclusive J/ψ sample. The event yield after the efficiency correction is

$$N_{J/\psi J/\psi}^{\text{corr}} = 672 \pm 129.$$

The cross-section for double J/ψ production in the fiducial range $2 < y_{J/\psi} < 4.5$ and $p_{\text{T}}^{J/\psi} < 10 \text{ GeV}/c$ is computed as

$$\sigma_{J/\psi J/\psi} = \frac{N_{J/\psi J/\psi}^{\text{corr}}}{\mathcal{L} \times \mathcal{B}_{\mu^+\mu^-}^2},$$

where $\mathcal{L} = 37.5 \pm 1.3 \text{ pb}^{-1}$ is the integrated luminosity and $\mathcal{B}_{\mu^+\mu^-} = (5.93 \pm 0.06)\%$ [39] is the J/ψ → μ⁺μ⁻ branching ratio. The result is

$$\sigma_{J/\psi J/\psi} = 5.1 \pm 1.0 \pm 1.1 \text{ nb},$$

where the first uncertainty is statistical and the second systematic.

Using the measured prompt J/ψ production cross-section in the same fiducial region [32] and taking into account the correlated uncertainties, the ratio of cross-sections $\sigma_{J/\psi J/\psi} / \sigma_{J/\psi}$ is calculated to be

$$\sigma_{J/\psi J/\psi} / \sigma_{J/\psi} = (5.1 \pm 1.0 \pm 0.6_{-1.0}^{+1.2}) \times 10^{-4},$$

where the first error is statistical, the second systematic and the third is due to the unknown polarisation of the prompt J/ψ and J/ψ from pair production.

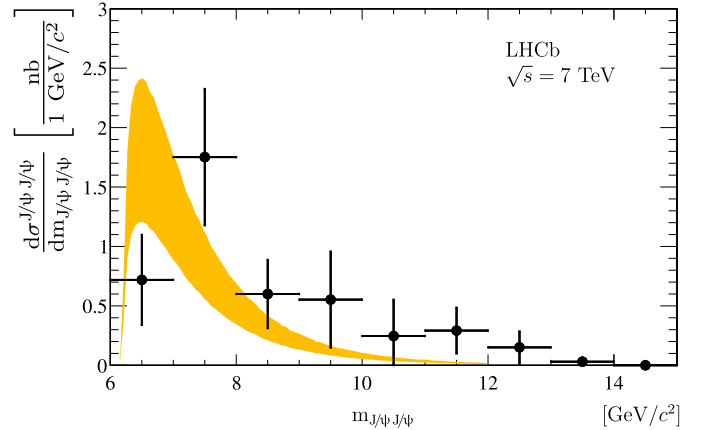


Fig. 2. Differential production cross-section for J/ψ pairs as a function of the invariant mass of the J/ψJ/ψ system. The points correspond to the data. Only statistical uncertainties are included in the error bars. The shaded area corresponds to prediction by the model described in Ref. [20].

The differential production cross-section of J/ψ pairs as a function of the invariant mass of the J/ψJ/ψ system is shown in Fig. 2. The whole analysis chain has been repeated for each bin of J/ψJ/ψ invariant mass to get the differential production cross-section. The bulk of the distribution is concentrated in the low invariant mass region. A theoretical prediction for the shape of this distribution taking into account both direct production and feeddown from ψ(2S) decays [20] is overlaid. Within the available statistics the agreement between the data and the prediction is reasonable.

7. Conclusions

The production of J/ψ pairs in proton–proton collisions at a centre-of-mass energy of 7 TeV has been observed with a statistical significance in excess of 6σ. The data are consistent with the predictions given in Refs. [19,20]. The higher statistics that will be collected during the 2011 data-taking period will allow the kinematic properties of these events to be studied and different production models to be probed.

Acknowledgements

We would like to thank A.K. Likhoded for many fruitful discussions. We express our gratitude to our colleagues in the CERN accelerator departments for the excellent performance of the LHC. We thank the technical and administrative staff at CERN and at the LHCb institutes, and acknowledge support from the National Agencies: CAPES, CNPq, FAPERJ and FINEP (Brazil); CERN; NSFC (China); CNRS/IN2P3 (France); BMBF, DFG, HGF and MPG (Germany); SFI (Ireland); INFN (Italy); FOM and NWO (Netherlands); SCSR (Poland); ANCS (Romania); MinES of Russia and Rosatom (Russia); MICINN, XuntaGal and GENCAT (Spain); SNSF and SER (Switzerland); NAS Ukraine (Ukraine); STFC (United Kingdom); NSF (USA). We also acknowledge the support received from the ERC under FP7 and the Region Auvergne.

Open access

This article is published Open Access at sciencedirect.com. It is distributed under the terms of the Creative Commons Attribution License 3.0, which permits unrestricted use, distribution, and reproduction in any medium, provided the original authors and source are credited.

References

- [1] V.G. Kartvelishvili, A.K. Likhoded, S.R. Slabospitsky, *Sov. J. Nucl. Phys.* 28 (1978) 678;
V.G. Kartvelishvili, A.K. Likhoded, S.R. Slabospitsky, *Yad. Fiz.* 28 (1978) 1315.
- [2] E.L. Berger, D.L. Jones, *Phys. Rev. D* 23 (1981) 1521.
- [3] R. Baier, R. Ruckl, *Phys. Lett. B* 102 (1981) 364.
- [4] F. Abe, et al., *Phys. Rev. Lett.* 69 (1992) 3704.
- [5] E. Braaten, S. Fleming, *Phys. Rev. Lett.* 74 (1995) 3327.
- [6] J.M. Campbell, F. Maltoni, F. Tramontano, *Phys. Rev. Lett.* 98 (2007) 252002.
- [7] B. Gong, J.X. Wang, *Phys. Rev. Lett.* 100 (2008) 232001.
- [8] P. Artoisenet, J.M. Campbell, J.-P. Lansberg, F. Maltoni, F. Tramontano, *Phys. Rev. Lett.* 101 (2008) 152001.
- [9] J.-P. Lansberg, *Eur. Phys. J. C* 61 (2009) 693.
- [10] N. Brambilla, et al., *Eur. Phys. J. C* 71 (2011) 1534.
- [11] C.H. Kom, A. Kulesza, W.J. Stirling, *Phys. Rev. Lett.* 107 (2011) 092002.
- [12] S.P. Baranov, A.M. Snigirev, N.P. Zotov, *Phys. Lett. B* 705 (2011) 116.
- [13] A. Novoselov, Double parton scattering as a source of quarkonia pairs in LHCb, arXiv:1106.2184 [hep-ph].
- [14] J. Badier, et al., *Phys. Lett. B* 114 (1982) 457.
- [15] J. Badier, et al., *Phys. Lett. B* 158 (1985) 85.
- [16] V.G. Kartvelishvili, S.M. Esakiya, *Yad. Fiz.* 38 (1983) 722.
- [17] B. Humpert, P. Mery, *Z. Phys. C* 20 (1983) 83.
- [18] V.V. Kiselev, A.K. Likhoded, S.R. Slabospitsky, A.V. Tkabladze, *Sov. J. Nucl. Phys.* 49 (1989) 1041;
V.V. Kiselev, A.K. Likhoded, S.R. Slabospitsky, A.V. Tkabladze, *Yad. Fiz.* 49 (1989) 1681.
- [19] C.F. Qiao, L.P. Sun, P. Sun, *J. Phys. G* 37 (2010) 075019.
- [20] A.V. Berezhnoy, A.K. Likhoded, A.V. Luchinsky, A.A. Novoselov, *Phys. Rev. D* 84 (2011) 094023.
- [21] A.A. Alves, et al., *JINST* 3 (2008) S08005.
- [22] T. Sjöstrand, S. Mrenna, P.Z. Skands, *JHEP* 0605 (2006) 026, arXiv:hep-ph/0603175.
- [23] I. Belyaev, et al., Handling of the generation of primary events in Gauss, the LHCb simulation framework, in: Nuclear Science Symposium Conference Record (NSS/MIC), IEEE, 2010, p. 1155.
- [24] D. Lange, *Nucl. Instrum. Meth. A* 462 (2001) 152.
- [25] S. Agostinelli, et al., *Nucl. Instrum. Meth. A* 506 (2003) 250.
- [26] A. Powell, Particle identification at LHCb, in: PoS ICHEP2010, 020, 2010.
- [27] S. Kullback, R.A. Leibler, *Ann. Math. Stat.* 22 (1951) 79;
S. Kullback, *Amer. Statist.* 41 (1987) 340.
- [28] W.D. Hulsbergen, *Nucl. Instrum. Meth. A* 552 (2005) 566.
- [29] J.E. Gaiser, Charmonium spectroscopy from radiative decays of the J/ψ and ψ' , PhD thesis, SLAC-R-255, 1982.
- [30] T. Skwarnicki, A study of the radiative cascade transitions between the Υ' and Υ resonances, PhD thesis, DESY-F31-86-02, 1986.
- [31] R. Aaij, et al., *Phys. Lett. B* 699 (2011) 330.
- [32] R. Aaij, et al., *Eur. Phys. J. C* 71 (2011) 1645.
- [33] E. Lópes Azamar, et al., Measurement of trigger efficiencies and biases, CERN-LHCb-2008-073, 2008.
- [34] R. Aaij, et al., *Phys. Lett. B* 693 (2010) 69.
- [35] S. van der Meer, Calibration of the effective beam height in the ISR, ISR-PO/68-31, 1968.
- [36] M. Ferro-Luzzi, *Nucl. Instrum. Meth. A* 553 (2005) 388.
- [37] G. Anders, et al., LHC bunch current normalization for the October 2010 luminosity calibration measurements, CERN-ATS-Note-2011-016 PERF, 2011.
- [38] R. Aaij, et al., Absolute luminosity measurements with the LHCb detector at the LHC, LHCb-PAPER-2011-015, CERN-PH-EP-2011-157, arXiv:1110.2866, JINST, submitted for publication.
- [39] K. Nakamura, et al., *J. Phys. G* 37 (2010) 075021.

LHCb Collaboration

R. Aaij²³, B. Adeva³⁶, M. Adinolfi⁴², C. Adrover⁶, A. Affolder⁴⁸, Z. Ajaltouni⁵, J. Albrecht³⁷, F. Alessio³⁷, M. Alexander⁴⁷, G. Alkhazov²⁹, P. Alvarez Cartelle³⁶, A.A. Alves Jr.²², S. Amato², Y. Amhis³⁸, J. Anderson³⁹, R.B. Appleby⁵⁰, O. Aquines Gutierrez¹⁰, F. Archilli^{18,37}, L. Arrabito⁵³, A. Artamonov³⁴, M. Artuso^{52,37}, E. Aslanides⁶, G. Auriemma^{22,m}, S. Bachmann¹¹, J.J. Back⁴⁴, D.S. Bailey⁵⁰, V. Balagura^{30,37}, W. Baldini¹⁶, R.J. Barlow⁵⁰, C. Barschel³⁷, S. Barsuk⁷, W. Barter⁴³, A. Bates⁴⁷, C. Bauer¹⁰, Th. Bauer²³, A. Bay³⁸, I. Bediaga¹, K. Belous³⁴, I. Belyaev^{30,37,*}, E. Ben-Haim⁸, M. Benayoun⁸, G. Bencivenni¹⁸, S. Benson⁴⁶, J. Benton⁴², R. Bernet³⁹, M.-O. Bettler¹⁷, M. van Beuzekom²³, A. Bien¹¹, S. Bifani¹², A. Bizzeti^{17,h}, P.M. Bjørnstad⁵⁰, T. Blake⁴⁹, F. Blanc³⁸, C. Blanks⁴⁹, J. Blouw¹¹, S. Blusk⁵², A. Bobrov³³, V. Bocci²², A. Bondar³³, N. Bondar²⁹, W. Bonivento¹⁵, S. Borghi⁴⁷, A. Borgia⁵², T.J.V. Bowcock⁴⁸, C. Bozzi¹⁶, T. Brambach⁹, J. van den Brand²⁴, J. Bressieux³⁸, D. Brett⁵⁰, S. Brisbane⁵¹, M. Britsch¹⁰, T. Britton⁵², N.H. Brook⁴², H. Brown⁴⁸, A. Büchler-Germann³⁹, I. Burducea²⁸, A. Bursche³⁹, J. Buytaert³⁷, S. Cadeddu¹⁵, J.M. Caicedo Carvajal³⁷, O. Callot⁷, M. Calvi^{20,j}, M. Calvo Gomez^{35,n}, A. Camboni³⁵, P. Campana^{18,37}, A. Carbone¹⁴, G. Carboni^{21,k}, R. Cardinale^{19,37,i}, A. Cardini¹⁵, L. Carson³⁶, K. Carvalho Akiba²³, G. Casse⁴⁸, M. Cattaneo³⁷, M. Charles⁵¹, Ph. Charpentier³⁷, N. Chiapolini³⁹, K. Ciba³⁷, X. Cid Vidal³⁶, G. Ciezarek⁴⁹, P.E.L. Clarke^{46,37}, M. Clemencic³⁷, H.V. Cliff⁴³, J. Closier³⁷, C. Coca²⁸, V. Coco²³, J. Cogan⁶, P. Collins³⁷, F. Constantin²⁸, G. Conti³⁸, A. Contu⁵¹, A. Cook⁴², M. Coombes⁴², G. Corti³⁷, G.A. Cowan³⁸, R. Currie⁴⁶, B. D'Almagne⁷, C. D'Ambrosio³⁷, P. David⁸, I. De Bonis⁴, S. De Capua^{21,k}, M. De Cian³⁹, F. De Lorenzi¹², J.M. De Miranda¹, L. De Paula², P. De Simone¹⁸, D. Decamp⁴, M. Deckenhoff⁹, H. Degaudenzi^{38,37}, M. Deissenroth¹¹, L. Del Buono⁸, C. Deplano¹⁵, O. Deschamps⁵, F. Dettori^{15,d}, J. Dickens⁴³, H. Dijkstra³⁷, P. Diniz Batista¹, S. Donleavy⁴⁸, A. Dosil Suárez³⁶, D. Dossett⁴⁴, A. Dovbnya⁴⁰, F. Dupertuis³⁸, R. Dzhelyadin³⁴, C. Eames⁴⁹, S. Easo⁴⁵, U. Egede⁴⁹, V. Egorychev³⁰, S. Eidelman³³, D. van Eijk²³, F. Eisele¹¹, S. Eisenhardt⁴⁶, R. Ekelhof⁹, L. Eklund⁴⁷, Ch. Elsasser³⁹, D.G. d'Enterria^{35,o}, D. Esperante Pereira³⁶, L. Estève⁴³, A. Falabella^{16,e}, E. Fanchini^{20,j}, C. Färber¹¹, G. Fardell⁴⁶, C. Farinelli²³, S. Farry¹², V. Fave³⁸, V. Fernandez Albor³⁶, M. Ferro-Luzzi³⁷, S. Filippov³², C. Fitzpatrick⁴⁶, M. Fontana¹⁰, F. Fontanelli^{19,i}, R. Forty³⁷, M. Frank³⁷, C. Frei³⁷, M. Frosini^{17,37,f}, S. Furcas²⁰, A. Gallas Torreira³⁶, D. Galli^{14,c}, M. Gandelman², P. Gandini⁵¹, Y. Gao³, J.-C. Garnier³⁷, J. Garofoli⁵², J. Garra Tico⁴³, L. Garrido³⁵, C. Gaspar³⁷, N. Gauvin³⁸, M. Gersabeck³⁷, T. Gershon^{44,37}, Ph. Ghez⁴, V. Gibson⁴³, V.V. Gligorov³⁷, C. Göbel⁵⁴, D. Golubkov³⁰, A. Golutvin^{49,30,37}, A. Gomes²,

H. Gordon⁵¹, M. Grabalosa Gándara³⁵, R. Graciani Diaz³⁵, L.A. Granado Cardoso³⁷, E. Graugés³⁵, G. Graziani¹⁷, A. Grecu²⁸, S. Gregson⁴³, B. Gui⁵², E. Gushchin³², Yu. Guz³⁴, T. Gys³⁷, G. Haefeli³⁸, C. Haen³⁷, S.C. Haines⁴³, T. Hampson⁴², S. Hansmann-Menzemer¹¹, R. Harji⁴⁹, N. Harnew⁵¹, J. Harrison⁵⁰, P.F. Harrison⁴⁴, J. He⁷, V. Heijne²³, K. Hennessy⁴⁸, P. Henrard⁵, J.A. Hernando Morata³⁶, E. van Herwijnen³⁷, E. Hicks⁴⁸, W. Hofmann¹⁰, K. Holubyev¹¹, P. Hopchev⁴, W. Hulsbergen²³, P. Hunt⁵¹, T. Huse⁴⁸, R.S. Huston¹², D. Hutchcroft⁴⁸, D. Hynds⁴⁷, V. Iakovenko⁴¹, P. Ilten¹², J. Imong⁴², R. Jacobsson³⁷, A. Jaeger¹¹, M. Jahjah Hussein⁵, E. Jans²³, F. Jansen²³, P. Jaton³⁸, B. Jean-Marie⁷, F. Jing³, M. John⁵¹, D. Johnson⁵¹, C.R. Jones⁴³, B. Jost³⁷, S. Kandybei⁴⁰, M. Karacson³⁷, T.M. Karbach⁹, J. Keaveney¹², U. Kerzel³⁷, T. Ketel²⁴, A. Keune³⁸, B. Khanji⁶, Y.M. Kim⁴⁶, M. Knecht³⁸, S. Koblitz³⁷, P. Koppenburg²³, A. Kozlinskiy²³, L. Kravchuk³², K. Kreplin¹¹, M. Kreps⁴⁴, G. Krocker¹¹, P. Krokovny¹¹, F. Kruse⁹, K. Krzuelecki³⁷, M. Kucharczyk^{20,25,37}, S. Kukulak²⁵, R. Kumar^{14,37}, T. Kvaratskheliya^{30,37}, V.N. La Thi³⁸, D. Lacarrere³⁷, G. Lafferty⁵⁰, A. Lai¹⁵, D. Lambert⁴⁶, R.W. Lambert³⁷, E. Lanciotti³⁷, G. Lanfranchi¹⁸, C. Langenbruch¹¹, T. Latham⁴⁴, R. Le Gac⁶, J. van Leerdam²³, J.-P. Lees⁴, R. Lefèvre⁵, A. Leflat^{31,37}, J. Lefrançois⁷, O. Leroy⁶, T. Lesiak²⁵, L. Li³, L. Li Gioi⁵, M. Lieng⁹, M. Liles⁴⁸, R. Lindner³⁷, C. Linn¹¹, B. Liu³, G. Liu³⁷, J.H. Lopes², E. Lopez Asamar³⁵, N. Lopez-March³⁸, J. Luisier³⁸, F. Machefert⁷, I.V. Machikhiliyan^{4,30}, F. Maciuc¹⁰, O. Maev^{29,37}, J. Magnin¹, S. Malde⁵¹, R.M.D. Mamunur³⁷, G. Manca^{15,d}, G. Mancinelli⁶, N. Mangiafave⁴³, U. Marconi¹⁴, R. Märki³⁸, J. Marks¹¹, G. Martellotti²², A. Martens⁷, L. Martin⁵¹, A. Martín Sánchez⁷, D. Martinez Santos³⁷, A. Massafferri¹, Z. Mathe¹², C. Matteuzzi²⁰, M. Matveev²⁹, E. Maurice⁶, B. Maynard⁵², A. Mazurov^{32,16,37}, G. McGregor⁵⁰, R. McNulty¹², C. Mclean¹⁴, M. Meissner¹¹, M. Merk²³, J. Merkel⁹, R. Messi^{21,k}, S. Miglioranza³⁷, D.A. Milanes^{13,37}, M.-N. Minard⁴, S. Monteil⁵, D. Moran¹², P. Morawski²⁵, R. Mountain⁵², I. Mous²³, F. Muheim⁴⁶, K. Müller³⁹, R. Muresan^{28,38}, B. Muryn²⁶, M. Musy³⁵, J. Mylroie-Smith⁴⁸, P. Naik⁴², T. Nakada³⁸, R. Nandakumar⁴⁵, J. Nardulli⁴⁵, I. Nasteva¹, M. Nedos⁹, M. Needham⁴⁶, N. Neufeld³⁷, C. Nguyen-Mau^{38,p}, M. Nicol⁷, S. Nies⁹, V. Niess⁵, N. Nikitin³¹, A. Novoselov³⁴, A. Oblakowska-Mucha²⁶, V. Obraztsov³⁴, S. Oggero²³, S. Ogilvy⁴⁷, O. Okhrimenko⁴¹, R. Oldeman^{15,d}, M. Orlandea²⁸, J.M. Otalora Goicochea², P. Owen⁴⁹, B. Pal⁵², J. Palacios³⁹, M. Palutan¹⁸, J. Panman³⁷, A. Papanestis⁴⁵, M. Pappagallo^{13,b}, C. Parkes^{47,37}, C.J. Parkinson⁴⁹, G. Passaleva¹⁷, G.D. Patel⁴⁸, M. Patel⁴⁹, S.K. Paterson⁴⁹, G.N. Patrick⁴⁵, C. Patrignani^{19,i}, C. Pavel-Nicorescu²⁸, A. Pazos Alvarez³⁶, A. Pellegrino²³, G. Penso^{22,l}, M. Pepe Altarelli³⁷, S. Perazzini^{14,c}, D.L. Perego^{20,j}, E. Perez Trigo³⁶, A. Pérez-Calero Yzquierdo³⁵, P. Perret⁵, M. Perrin-Terrin⁶, G. Pessina²⁰, A. Petrella^{16,37}, A. Petrolini^{19,i}, B. Pie Valls³⁵, B. Pietrzyk⁴, T. Pilar⁴⁴, D. Pinci²², R. Plackett⁴⁷, S. Playfer⁴⁶, M. Plo Casasus³⁶, G. Polok²⁵, A. Poluektov^{44,33}, E. Polcarpo², D. Popov¹⁰, B. Popovici²⁸, C. Potterat³⁵, A. Powell⁵¹, T. du Pree²³, J. Prisciandaro³⁸, V. Pugatch⁴¹, A. Puig Navarro³⁵, W. Qian⁵², J.H. Rademacker⁴², B. Rakotomiramanana³⁸, M.S. Rangel², I. Raniuk⁴⁰, G. Raven²⁴, S. Redford⁵¹, M.M. Reid⁴⁴, A.C. dos Reis¹, S. Ricciardi⁴⁵, K. Rinnert⁴⁸, D.A. Roa Romero⁵, P. Robbe⁷, E. Rodrigues⁴⁷, F. Rodrigues², P. Rodriguez Perez³⁶, G.J. Rogers⁴³, S. Roiser³⁷, V. Romanovsky³⁴, J. Rouvinet³⁸, T. Ruf³⁷, H. Ruiz³⁵, G. Sabatino^{21,k}, J.J. Saborido Silva³⁶, N. Sagidova²⁹, P. Sail⁴⁷, B. Saitta^{15,d}, C. Salzmann³⁹, M. Sannino^{19,i}, R. Santacesaria²², R. Santinelli³⁷, E. Santovetti^{21,k}, M. Sapunov⁶, A. Sarti^{18,l}, C. Satriano^{22,m}, A. Satta²¹, M. Savrie^{16,e}, D. Savrina³⁰, P. Schaack⁴⁹, M. Schiller¹¹, S. Schleich⁹, M. Schmelling¹⁰, B. Schmidt³⁷, O. Schneider³⁸, A. Schopper³⁷, M.-H. Schune⁷, R. Schwemmer³⁷, A. Sciubba^{18,l}, M. Seco³⁶, A. Semennikov³⁰, K. Senderowska²⁶, I. Sepp⁴⁹, N. Serra³⁹, J. Serrano⁶, P. Seyfert¹¹, B. Shao³, M. Shapkin³⁴, I. Shapoval^{40,37}, P. Shatalov³⁰, Y. Shcheglov²⁹, T. Shears⁴⁸, L. Shekhtman³³, O. Shevchenko⁴⁰, V. Shevchenko³⁰, A. Shires⁴⁹, R. Silva Coutinho⁵⁴, H.P. Skottowe⁴³, T. Skwarnicki⁵², A.C. Smith³⁷, N.A. Smith⁴⁸, K. Sobczak⁵, F.J.P. Soler⁴⁷, A. Solomin⁴², F. Soomro⁴⁹, B. Souza De Paula², B. Spaan⁹, A. Sparkes⁴⁶, P. Spradlin⁴⁷, F. Stagni³⁷, S. Stahl¹¹, O. Steinkamp³⁹, S. Stoica²⁸, S. Stone^{52,37}, B. Storaci²³, M. Straticiu²⁸, U. Straumann³⁹, N. Styles⁴⁶, V.K. Subbiah³⁷, S. Swientek⁹, M. Szczekowski²⁷, P. Szczypka³⁸, T. Szumlak²⁶, S. T'Jampens⁴, E. Teodorescu²⁸, F. Teubert³⁷, C. Thomas^{51,45}, E. Thomas³⁷, J. van Tilburg¹¹, V. Tisserand⁴, M. Tobin³⁹, S. Topp-Joergensen⁵¹, M.T. Tran³⁸, A. Tsaregorodtsev⁶, N. Tuning²³, A. Ukleja²⁷, P. Urquijo⁵², U. Uwer¹¹, V. Vagnoni¹⁴, G. Valenti¹⁴, R. Vazquez Gomez³⁵, P. Vazquez Regueiro³⁶, S. Vecchi¹⁶, J.J. Velthuis⁴², M. Veltri^{17,g}, K. Vervink³⁷, B. Viaud⁷, I. Videau⁷, X. Vilasis-Cardona^{35,n}, J. Visniakov³⁶, A. Vollhardt³⁹, D. Voong⁴², A. Vorobyev²⁹, H. Voss¹⁰, K. Wacker⁹,

S. Wandernoth¹¹, J. Wang⁵², D.R. Ward⁴³, A.D. Webber⁵⁰, D. Websdale⁴⁹, M. Whitehead⁴⁴,
 D. Wiedner¹¹, L. Wiggers²³, G. Wilkinson⁵¹, M.P. Williams^{44,45}, M. Williams⁴⁹, F.F. Wilson⁴⁵,
 J. Wishahi⁹, M. Witek^{25,37}, W. Witzeling³⁷, S.A. Wotton⁴³, K. Wyllie³⁷, Y. Xie⁴⁶, F. Xing⁵¹, Z. Yang³,
 R. Young⁴⁶, O. Yushchenko³⁴, M. Zavertyaev^{10,a}, L. Zhang⁵², W.C. Zhang¹², Y. Zhang³, A. Zhelezov¹¹,
 L. Zhong³, E. Zverev³¹, A. Zvyagin³⁷

¹ Centro Brasileiro de Pesquisas Físicas (CBPF), Rio de Janeiro, Brazil

² Universidade Federal do Rio de Janeiro (UFRJ), Rio de Janeiro, Brazil

³ Center for High Energy Physics, Tsinghua University, Beijing, China

⁴ LAPP, Université de Savoie, CNRS/IN2P3, Annecy-Le-Vieux, France

⁵ Clermont Université, Université Blaise Pascal, CNRS/IN2P3, LPC, Clermont-Ferrand, France

⁶ CPPM, Aix-Marseille Université, CNRS/IN2P3, Marseille, France

⁷ LAL, Université Paris-Sud, CNRS/IN2P3, Orsay, France

⁸ LPNHE, Université Pierre et Marie Curie, Université Paris Diderot, CNRS/IN2P3, Paris, France

⁹ Fakultät Physik, Technische Universität Dortmund, Dortmund, Germany

¹⁰ Max-Planck-Institut für Kernphysik (MPIK), Heidelberg, Germany

¹¹ Physikalisches Institut, Ruprecht-Karls-Universität Heidelberg, Heidelberg, Germany

¹² School of Physics, University College Dublin, Dublin, Ireland

¹³ Sezione INFN di Bari, Bari, Italy

¹⁴ Sezione INFN di Bologna, Bologna, Italy

¹⁵ Sezione INFN di Cagliari, Cagliari, Italy

¹⁶ Sezione INFN di Ferrara, Ferrara, Italy

¹⁷ Sezione INFN di Firenze, Firenze, Italy

¹⁸ Laboratori Nazionali dell'INFN di Frascati, Frascati, Italy

¹⁹ Sezione INFN di Genova, Genova, Italy

²⁰ Sezione INFN di Milano Bicocca, Milano, Italy

²¹ Sezione INFN di Roma Tor Vergata, Roma, Italy

²² Sezione INFN di Roma La Sapienza, Roma, Italy

²³ Nikhef National Institute for Subatomic Physics, Amsterdam, Netherlands

²⁴ Nikhef National Institute for Subatomic Physics and Vrije Universiteit, Amsterdam, Netherlands

²⁵ Henryk Niewodniczanski Institute of Nuclear Physics Polish Academy of Sciences, Cracow, Poland

²⁶ Faculty of Physics & Applied Computer Science, Cracow, Poland

²⁷ Soltan Institute for Nuclear Studies, Warsaw, Poland

²⁸ Horia Hulubei National Institute of Physics and Nuclear Engineering, Bucharest-Magurele, Romania

²⁹ Petersburg Nuclear Physics Institute (PNPI), Gatchina, Russia

³⁰ Institute of Theoretical and Experimental Physics (ITEP), Moscow, Russia

³¹ Institute of Nuclear Physics, Moscow State University (SINP MSU), Moscow, Russia

³² Institute for Nuclear Research of the Russian Academy of Sciences (INR RAN), Moscow, Russia

³³ Budker Institute of Nuclear Physics (SB RAS) and Novosibirsk State University, Novosibirsk, Russia

³⁴ Institute for High Energy Physics (IHEP), Protvino, Russia

³⁵ Universitat de Barcelona, Barcelona, Spain

³⁶ Universidad de Santiago de Compostela, Santiago de Compostela, Spain

³⁷ European Organization for Nuclear Research (CERN), Geneva, Switzerland

³⁸ Ecole Polytechnique Fédérale de Lausanne (EPFL), Lausanne, Switzerland

³⁹ Physik-Institut, Universität Zürich, Zürich, Switzerland

⁴⁰ NSC Kharkiv Institute of Physics and Technology (NSC KIPT), Kharkiv, Ukraine

⁴¹ Institute for Nuclear Research of the National Academy of Sciences (KINR), Kyiv, Ukraine

⁴² H.H. Wills Physics Laboratory, University of Bristol, Bristol, United Kingdom

⁴³ Cavendish Laboratory, University of Cambridge, Cambridge, United Kingdom

⁴⁴ Department of Physics, University of Warwick, Coventry, United Kingdom

⁴⁵ STFC Rutherford Appleton Laboratory, Didcot, United Kingdom

⁴⁶ School of Physics and Astronomy, University of Edinburgh, Edinburgh, United Kingdom

⁴⁷ School of Physics and Astronomy, University of Glasgow, Glasgow, United Kingdom

⁴⁸ Oliver Lodge Laboratory, University of Liverpool, Liverpool, United Kingdom

⁴⁹ Imperial College London, London, United Kingdom

⁵⁰ School of Physics and Astronomy, University of Manchester, Manchester, United Kingdom

⁵¹ Department of Physics, University of Oxford, Oxford, United Kingdom

⁵² Syracuse University, Syracuse, NY, United States

⁵³ CC-IN2P3, CNRS/IN2P3, Lyon-Villeurbanne, France^q

⁵⁴ Pontifícia Universidade Católica do Rio de Janeiro (PUC-Rio), Rio de Janeiro, Brazil^r

* Corresponding author at: Institute of Theoretical and Experimental Physics (ITEP), Moscow, Russia.

E-mail address: Ivan.Belyaev@itep.ru (I. Belyaev).

^a P.N. Lebedev Physical Institute, Russian Academy of Science (LPI RAS), Moscow, Russia.

^b Università di Bari, Bari, Italy.

^c Università di Bologna, Bologna, Italy.

^d Università di Cagliari, Cagliari, Italy.

^e Università di Ferrara, Ferrara, Italy.

^f Università di Firenze, Firenze, Italy.

^g Università di Urbino, Urbino, Italy.

^h Università di Modena e Reggio Emilia, Modena, Italy.

ⁱ Università di Genova, Genova, Italy.

^j Università di Milano Bicocca, Milano, Italy.

^k Università di Roma Tor Vergata, Roma, Italy.

^l Università di Roma La Sapienza, Roma, Italy.

- ^m Università della Basilicata, Potenza, Italy.
- ⁿ LIFAELS, La Salle, Universitat Ramon Llull, Barcelona, Spain.
- ^o Institució Catalana de Recerca i Estudis Avançats (ICREA), Barcelona, Spain.
- ^p Hanoi University of Science, Hanoi, Viet Nam.
- ^q Associated member.
- ^r Associated to Universidade Federal do Rio de Janeiro (UFRJ), Rio de Janeiro, Brazil.